
Article:
Goode, J orcid.org/0000-0002-3642-1291, Dillon, G and Millner, PA orcid.org/0000-0002-4813-4302 (2016) The development and optimisation of Nanobody based electrochemical immunosensors for IgG. Sensors and Actuators B: Chemical, 234. pp. 478-484. ISSN 0925-4005

https://doi.org/10.1016/j.snb.2016.04.132

The development and optimisation of Nanobody based electrochemical immunosensors for IgG.

J.Goode*[1, 2], G.Dillon[2], P.A.Millner[1]

[1]School of Biomedical Sciences, Faculty of Biological Sciences, University of Leeds, UK

[2]Abcam Plc. 204 Cambridge Science Park, Cambridge, CB4 0GZ, UK

*J.A.Goode@leeds.ac.uk *Tel: (+44)113 34 34272*

Abstract

Biosensors are increasingly heralded for their potential to create inexpensive diagnostic devices which are sensitive, selective and easy to use. One of the key categories of biosensor are immunosensors, which have historically used antibodies as bioreceptors. Though widely used, antibodies bring inherent limitations such as variability, limited stability and their reliance on animal sources.

This has led to the development of alternative immuno-reagents such as non-antibody binding proteins (NABPs). These are low molecular weight proteins which largely avoid the aforementioned advantages of antibodies. They are commonly produced by bacteria enabling the use of DNA technology to manipulate bioreceptors at the molecular level.

Single chain VHHs (commonly known as nanobodies) are an antibody derived NABP adapted from camelid heavy chain antibodies which are the isolated binding domain. Whilst nanobodies have been used for diagnostic and therapeutic applications, they have limited demonstration in biosensors.

In this study, both antibodies and nanobodies were used to construct a biosensor. In addition nanobody performance was optimised by introducing a novel peptide spacer. The role of nanobody orientation and spacing was thus investigated and spacer length was optimised, leading to an increase in the sensitivity of the biosensor.

Highlights:

- Nanobodies have been used on impedimetric immunosensors to detect rabbit IgG
- Unmodified nanobody sensors displayed a decrease in resistance upon analyte recognition.
- Nanobodies were modified with a peptide spacer, effectively reversing this phenomena.
- The use of a spacer also increased the sensitivity of the immunosensor.

Keywords:

Nanobody; Impedance; Immunosensor; Orientation; Spacer; Steric Hindrance

Abbreviations

NABP- Non antibody binding protein
V_{HH}-Hypervariable region
ScFv- Single Chain variable fragments
IgNAR- Immunoglobulin new antigen receptor

1. Introduction

A biosensor may be considered a three component system comprising: (a) the sample or analyte, (b) a transducer mechanism or bioreceptor and (c) a signal output. This report focuses on how altering the bioreceptor may be a crucial step in overcoming the barriers in the production of sensitive, low cost biosensors for both diagnostic and analytical applications. Though many sensors have been developed at the proof –of –concept level, there are only a few examples which have made the leap into the commercial market [1,2].

Most of the binding sensors developed to date rely on antibodies, the primary recognition agent of the immune system [3] and will be referred to as immunosensors throughout. Though antibodies are common reagents with well understood binding physics which allow the use of routine methods, there are a number of major drawbacks. These include batch to batch variability when using polyclonal antibodies, stability of the antibodies and their large size (150kDa) which precludes the possibility of protein engineering. Antibodies may also bring issues of cross reactivity which cannot be identified until after production. These technical shortcomings are in addition to the ethical issues raised by their reliance on animal use and the financial issues raised with their associated cost [4,5].

For these reasons, there is a movement towards the use of recombinant monoclonal antibodies and the use of non-antibody binding proteins (NABPs), the latter of which may be easily expressed using bacterial techniques which allow the continuous production of a stable protein with no variation.

Whilst this article focuses on the use of nanobodies, the lessons learned may support findings relevant to other types of NABP or engineered Fab fragments or single chain variable fragments (ScFvs). There are currently a number of candidate NABPs for biosensor development such as darpins [6] Adhirons [7] and affybodies [8]. Though the benefits of these receptors have been previously demonstrated using optical biosensor systems [9], there are limited reports on their application in electrochemical sensors and specifically a lack of data reported for impedimetric immunosensors [10]. There is no work to date focussing on both the orientation and inclusion of a peptide spacer to investigate the influence of bioreceptor height above the electrode on detection of analyte and signal generation.

The nanobody binding protein used in this study is an IgG fold domain which has been isolated from cammellid heavy chain only "Immunoglobulin New Antigen Receptors" (IgNARs). cDNA from lymphocytes was taken from immunised *Cammellidae* [11–13]. The cDNA can be sourced from lymphocytes isolated from blood taken from the host, avoiding animal sacrifice and contributing to the 3R's of animal use in research.

The cDNA extracted was isolated using PCR and used to construct a phage display library that could be screened to identify binding candidates for nanobody synthesis before sequencing and subcloning the DNA into a stable plasmid vector [14]. Screening can also be carried out at this stage to check for cross reactivity with candidate biomolecules which may commonly cross react with receptors [15]. This enables the elimination of receptors which cross react before the receptor is generated en-masse.

Once the DNA is ligated into a plasmid, it contains the sequence for a monoclonal-type binder and batch to batch variability is eliminated. This means that only one immunisation is necessary for a potentially endless source of nanobodies, producing a binder that is more reliable when compared

to polyclonal antibody production techniques, as well providing the potential for lower cost [16]. These benefits have enabled the development of novel [17–20], as well as showing early promise in the field of diagnostics [20,21].

The nanobody used in this report was engineered to include a His_6-Tag for easy purification. In addition the plasmid was further engineered to create nanobodies with an engineered peptide spacer of 5, 10 or 15 amino acids (a GGGGS motif repeated respectively) with a unique cysteine at the N-terminus to enable oriented conjugation of the receptor using thiol chemistry, the plasmids are summarised in **Appendix A**. Along with orientation, the use of spacers permitted the optimisation of receptor distance from the transducer surface, a parameter which may greatly impact the electrochemical signal generated.

Whilst the majority of reports aim to attach the bioreceptor intimately at biosensor interface, this may cause undesired effects such as a limitation in analyte binding due to steric hindrance. By providing a spatially coherent peptide spacer, these problems may be overcome as well as an improved degree of receptor orientation. The effect of steric hindrance has been demonstrated as a critical parameter in biosensor signal generation in previous studies [22–25]. It is hypothesised that the use of nanobodies will highlight the importance of orientation of the bioreceptor. As a comparison to the novel nanobody biosensors, data has been collected on antibody based biosensors; the variety of bioreceptors used in this study is illustrated in **Figure 1**.

The sensor constructed in the study was developed to specifically detect rabbit IgG, for the commercial demands of the antibody development industry. The sensor developed will provide an accessible method for assaying antibody concentration in both sera and in prepared antibody products. Currently, a multi-step procedure is needed to quantify rabbit IgG accurately, this is inefficient in terms of both time and resources as it often relies on relatively large sample volumes.

2. Materials & Methods

2.1. Expression and Purification of nanobodies.

A series of pHEN6 vectors was generated to create anti-rabbit IgG nanobodies, based on ab191866 (Abcam), the sequence was cloned into each modified pHEN6 vector using PstI and BstEII sites (Error! Reference source not found.) and modified vectors were generated by ligating in the sequence for include C-terminal spacers with a G4S motif (repeated for 5, 10 and 15 amino acid spacers with a terminal cysteine (Error! Reference source not found.) followed by a His_6-tag. This was achieved using BstEII and EcoRII sites. Following ligation, plasmids were transformed into WK6 *E.Coli* cultures using the heat shock method [26] and cultures were grown on Ampicillin containing TB–Agar plates pre-heated to 37 °C. Individual colonies were then picked and added to 5 ml LB–ampicillin media to form starter cultures. The following day, 2 ml of this culture as added to 500 ml LB–ampicillin and IPTG was used to induce cultures overnight.

Cells were collected by centrifugation at 3,000 x*g* for 30 min. The periplasm was then extracted using TES buffer (0.2M Tris-HCL 0.5M Sucrose 0.5mM EDTA) at 4 °C, shaking on ice for 1 hr. Finally, cell debris were collected by centrifugation at 6,800 x*g* for 5 min. The Periplasm extract was then purified on a Ni^{2+} chelating column as previously described [27] and imidazole was removed by dialysing the nanobody against PBS.

2.2. Reduction of nanobody dimers

The purified nanobody at 1 $mg.ml^{-1}$ was incubated with 50 mM 2-mercaptoethylamine (2-MEA), in degassed PBS plus 10 mM EDTA pH 7.4 for 90 min at 37 °C. This selectively reduced the disulfide bonds, reducing Nanobody dimers into monomers. Buffer exchange was then executed using Amicon®filters (3,000 MWCO) which were centrifuged at 14,000x*g* for 10 min to remove excess MEA. Buffer was replaced three times with previously degassed 1×PBS plus 10mM EDTA pH 7.4. Reduced nanobodies were then used immediately to prevent recombination of reduced nanobodies.

2.3. Immunoprecipitation

For immunoprecipitation studies, unmodified nanobodies were conjugated to N-Hydroxy succinimide (NHS) (GE Healthcare) and the modified nanobodies were conjugated to Sulfolink®(Sigma) sepharose beads according to manufacturers' protocols. Non-specific binding was reduced by blocking beads with glycine in the case of NHS beads and cysteine for Sulfolink beads (50mM cysteine in 50mM Tris-Hydroxymethylaminomethane plus 5Mm EDTA).

To confirm the affinity of the nanobodies had not been compromised, the beads were incubated with 100 µl diluted rabbit sera (10% v/v sera in PBS) for 2 hrs. After binding, a mild acid wash was performed using 100 mM sodium citrate (pH 4.0) and a final RIPA Buffer wash (50mM NaCl, 1%(v/v) IGEPAL CA-630®, 0.5%(w/v) sodium deoxycholate, 0.1%(w/v) SDS and 50 mM Tris, pH 8.0) to remove non-specifically bound protein from the beads.

For elution, a two stage procedure was employed. First, 100 mM glycine (pH 2.0) elution buffer was used to interrupt nanobody-antigen binding and elute bound analyte. Then, a second elution buffer containing PBS+ 100 mM DTT was used to liberate the modified nanobody from the Sulfolink®bead. This provided confirmation that the nanobody had bound via the engineered cysteine residue.

2.4. Identification of eluates

For identification, eluates from immunoprecipitation were subjected to non-reducing SDS-PAGE. Samples containing 1 µg protein in 8 µl running buffer [250mM Tris pH 7.6, 10% (w/v) SDS, 50% (v/v) glycerol, 0.01% (w/v) bromophenol blue (w/v)] were heated for 10 min at 70 °C and then added to pre-cast gels (4-12% acrylamide) (Invitrogen). Gels were run at 200 V for 50 min in 1x Trid-glycine running buffer. Following separation, the gels were either stained using Instant Blue® Coomassie stain, according to manufacturer's instruction or used for immunoblotting.

In immunoblot experiments, samples were transferred to nitrocellulose membrane at 30 V for 70 min in transfer buffer and transfer was confirmed using Ponceau-stain which was subsequently washed using TBST (20 mM Tris, 150 mM NaCl 0.1 % (v/v) Tween-20 pH 7.6). Membranes were then blocked using 5% (w/v) BSA in TBST before being probed with the appropriate HRP-antibody conjugates at 1:10,000 dilution in blocking buffer. Membranes were then washed thoroughly before adding ECL Substrate (SuperSignal®, Pierce) and imaging using a Syngene® G:Box System.

2.5. Biosensor construction and Bioreceptor Conjugation

2.5.1. Electrode Preparation

Customised DropSens® X2220AT gold electrodes were cleaned by ultra-sonication in 100 % ethanol for 10 min before rinsing in dH_2O and drying in a stream of argon. The working electrodes were then coated in a matrix of polytyramine by electropolymerising from a monomer solution (25 mM tyramine in 300 mM NaOH in MeOH) in accordance with previously established methods [28,29]. The solution was electrochemically polymerised onto the electrodes using cyclic voltammetry, with potential cycled between 0 V and 1.6 V (vs. Ag/AgCl) with a scan rate of 0.2 $V.s^{-1}$ for two consecutive scans data shown in (Appendix C), before equilibrating for 15 min in PBS pH 7.4.

2.5.2. Oriented conjugation of spacer modified nanobodies

The polymer modified electrodes were incubated with 5 mM sulfosuccinimidyl 4-[N-maleimidomethyl] cyclohexane-1-carboxylate (Sulfo-SMCC, **Sigma**) solution in 10 mM PBS-EDTA (10mM) pH 7.2 for one hour, as described in previous papers [30]. Freshly reduced nanobodies (from 2.2) were then added to the sulfo-SMCC modified electrode and incubated for 1 hr. These electrodes were incubated for 30 min in PBS pH 7.4 to remove any non-specifically bound receptor. The sensors were interrogated electrochemically prior to analyte detection to obtain a baseline sensor signal.

2.5.3. Non-Oriented Conjugation of full antibodies and nanobodies

For non-oriented bioreceptor studies, the bioreceptor (either Goat anti –rabbit IgG, *ab 97047 (Abcam)* or the nanobody) was firstly biotinylated using biotin-XX-NHS (Merck Millipore) according to established protocols [31]. Biotinylated bioreceptors were then stored at -20 °C. After electrode preparation (**2.5.1**), 3 mM biotin-NHS in PBS (20% w/v DMSO) was made and 10 µl was added to the working electrode for 60 min. After copious washing, 1mM Neutravidin® was added to the electrode for 45 min before rinsing; then finally 10 µl of the biotinylated protein was added and incubated for 1 h. The electrodes were once again incubated for 30 min in PBS after sensor assembly and a baseline signal obtained.

2.6. Biosensor Interrogation

After sensor assembly, electrochemical impedance spectroscopy (EIS) was used to monitor analyte recognition. Data was processed using NOVA software on a FRA-2 µAUTOLAB type III electrochemical workstation. The impedance analysis was performed over a frequency range from 0.25 Hz to 25 kHz, using a modulation voltage of ±10 mV at an applied voltage of 0.0V with respect to the reference electrode. All impedance experiments were performed in an electrolyte solution of 10 mM $K_3[Fe(CN)_6]$/ $K_4[Fe(CN)_6]$ (1:1 ratio) in 1xPBS, pH 7.4. Fully fabricated immunosensors were incubated with 10 µl analyte (rabbit anti sox- 9, ab26414 (***Abcam***)) at a concentration ranging from 666 fM to 666 nM for 30 min prior to sensor interrogation. The EIS response was read following copious rinsing of the analyte.

2.7. Data Analysis

Using Autolab NOVA Software, impedance data was modelled using a modified Randles' circuit in which the pure capacitor was replaced with a constant-phase element to simulate the non-ideal nature of capacitance at the biosensor surface[32] (**see Figure 4(B) inset**) . As the effects of Warburg impedance were not observed in the data, this component was also excluded from the model. Using this analysis, the simulated fit was found to have a deviation of 2.89 % ± 0.096 (n=64) from the measured data.

This fit generated values for Solution resistance (R_s), Charge Transfer resistance (R_{ct}) and constant-phase element (Q). For calibration of the biosensor R_{ct} was used as it was the most sensitive to analyte binding and is the most widely used measure for impedimetric analysis of biosensors in the field [32–36]. To ensure chip-to-chip variability was minimised, values were normalised to the initial baseline of the R_{CT} measured for the fully constructed sensor.

3 Results

3.1 Optimisation of synthesis and Dimer Reduction

Nanobodies were successfully expressed in *E.coli* before being purified. In nanobodies with engineered cysteine terminal receptors, dimers natively formed. These dimers were reduced by incubation with 2-MEA (90mM, 37 °C, 90 min). Confirmation of the purification and dimer reduction is illustrated in **Figure 2**. All lanes were run under non reducing conditions to ensure successful reduction of dimers could be observed. In all conditions the increasing molecular weight of the nanobodies can be observed, owing to the successful inclusion of the lengthening peptide spacer. The overall sample purity can also be clearly seen.

3.2 Immunoprecipitation of IgG from rabbit sera

Immunoprecipitation experiments illustrated that reduction had not denatured the nanobodies and that the use of the spacer had not interfered with the immune recognition of IgG by the nanobodies (**Figure 3**). In this figure the Coomassie of different elutions from the experiment is shown with corresponding blots for the analyte as well as the nanobody receptors.

Coomassie staining **Figure 3(A)** was done to assess the protein present in sera flow-through (s), glycine elution (gl) and DTT elution (dtt) of the immunoprecipitation experiments. Upon elution using glycine buffer bands can be observed at ~150 KDa corresponding to the molecular weight of IgG. When eluting with DTT bands are observed in the 12-15 KDa region, these correspond to the increasing molecular weight of the nanobody with their respective amino acid spacer.

The identity of these bands was confirmed in western blot; firstly using a goat-anti-rabbit –HRP conjugated antibody (***Dako*** *cat# P0448)* to identify the IgG band (**Figure 3(B)**). Secondly; an anti-His_6Tag –HRP conjugated antibody *(**Abcam** cat# ab1187)* was used to identify the nanobody, a band at 12-15KDa (**Figure 3(C)**). Across lanes, the signal is observed at increasing molecular weights corresponding to the 5, 10 and 15 amino acid peptide spacer modified nanobodies.

3.3 Biosensor Construction and Interrogation

Cyclic voltammetry (CV) verified the cleanliness and reproducibility of the gold surface before sensor construction (data not shown). Tyramine was then electrochemically polymerized on to the gold electrode in order to obtain a robust polymer with primary amino groups to permit functionalization of the sensor surface [29,37,38]. A characteristic cyclic voltammogram was seen across the two voltammetric cycles (Error! Reference source not found.), confirming the success of electropolymerisation.

After the polymer was equilibrated in PBS for 15 min, biosensors were constructed as described before interrogation. Impedance measurements were taken from 25 KHz-250 mHz and Nyquist plots were constructed. Nyquist data as in (**Figure 4)** was used to assess the binding. The difference between specific (**Figure 4(A)**) and non-specific signal (**Figure 4(B)**) can be seen in the nyquist data.

In order to allow cross comparison of the different nanobody biosensors with variable spacers against conventional antibody methods, R_{ct} was analysed by modelling the equivalent circuit displayed in **Figure 5, inset.** The R_{ct} was then used to calculate the average percent change compared with the initial sensor reading and construct a calibration. As sensors were interrogated suing specific rabbit IgG analyte and negative sheep IgG, a comparison of analyte specific signal obtained from different bioreceptor systems can be seen in **Figure 5.**

It can be seen from this data that when using IgG as a receptor, the addition of analyte causes an increase in the resistance across the sensor interface. This follows conventional findings in the development of impedimetric immunosensors [3,35,39,40], as the passing of ions across the interface is slowed upon anlyte binding, corresponding to an increase in effective resistance.

However, when using biotinylated nanobody as the receptor this is not the case. Instead a decrease in the resistnace is observed. To confirm this, controls were performed with negative and positive controls using another sensor (for GFP constructed using anti-GFP nanobodies, (ab192863,**Abcam**) (Error! Reference source not found.). This confirmed that the decrease in resitance is both analyte

dependent and observed consistently when using biotinylatyed nanobodies directly. This problem was successfully circumvented when using the oriented spacer.

From data in Figure 5 we can observe that the use of an oriented peptide spacer of five amino acids was the optimum as it generated a large signal and was more sensitive, still generating appreciable signal at the lowest concentration of anlyte (666 fM). Biosensors constructed using ten amino acid spacers generated signal which was comparable to that obtained when using IgG as a receptor. When using a receptor with a fifteen amino acid spacer however there was negligible generation of specific signal.

3.4 Optimisation of best candidate

As the biosensor constructed using a bioreceptor with five amino acid peptide spacer had been identified as the best candidate, this was taken forward to be interrogated using a full panel of controls (**Figure 6**) in relevant sampling media to mimic sera. The sensor was interrogated with in PBS as an ideal system as well as a negative control using sheep IgG, data for these experiments was used to obtain calibration from **Figure 5**. In addition to this, human sera at both 100 and 10 %v/v in PBS was spiked with the same rabbit IgG to ensure that the biosensor is operational in a relevant sampling matrix.

This demonstrated the successful detection of analyte in full sera and the overall specificity of the sensor in a complex media. Given that sera has a reference value of 60-80 mg.ml, an extremely high concertation when comparing to reference analyse range of the developed sensors , the sensor has proven successful. When using undiluted sera an inferior calibration was observed. This may be due to the very high concentrations of non-specific proteins in the sample suppressing generation of signal by the analyte. In this dataset, the highest concentration of analyte resulted in a sudden decrease of signal. This may be due to transducer or receptor disintegration given the repeated barrage of high concentration protein samples and the high number of incubation-interrogation cycles. The sample spiked in 10% sera is the most successful showing large signal generation. This represents a practical sampling method, where a commercial or medical sample would be diluted before application to the sensor.

4 Conclusion

In this study, an impedimetric immunosensor to rabbit IgG was fabricated using bespoke nanobody constructs as bioreceptors and compared to traditional antibody based biosensors.

When using conventional biosensor construction techniques with nanobodies, a negative calibration emerged, i.e. impedance fell on analyte binding which runs counter to most findings in this area. This trend was confirmed using a variety of controls and in the development of a similar sensor for green fluorescent protein (GFP). In both instances a change of ~40% in the Rct was observed.

A peptide spacer was engineered to resolve this issue which also brought the advantage of orienting the receptor on the biosensor surface. The inclusion of the peptide spacer rectified the impedance drop and allowed the effect of spacing to be investigated. Optimisation of spacer length altered the

signal and sensitivity of the sensor, leading to an improvement and a change of ~60% in the Rct to be observed. The optimal nanobody construct was observed with a peptide spacer of five amino acids. This sensor displayed reliable analyte specific signal down to pM analyte concentrations, demonstrating comparable sensitivity to established methods such as ELISA and superior performance to similar electrochemical biosensors [41,42]. As typical samples have μM concentrations, this biosensor has an appropriate functional range and allows for sample dilution which is beneficial for practical deployment.

In this study the spacer chosen had lengths of approximately 2, 4 and 6 nm which were compared to the solute layers present at the electrode interface. According to double layer theory and the Guoy-Chapman model [32], the typical length of the Debye layer at the electrode interface of this electrolyte system has a thickness of ~3 nm [32,43]. Using the five amino acid spacer therefore locates the receptor in the middle of the Debye layer. This may explain why the five amino acid spacer is optimal as longer spacers may place the receptor beyond the Debye layer, reducing the impedance signal generated upon analyte binding. The continued detection of analyte may be due to the spacer flexibility meaning that though the spacer length is greater than that of the Debye layer, it may flex and lead to some binding happening within the Debye layer. Along with the receptor being located optimally in the z-plane, the use of a five amino acid peptide spacer may also negate the effects of steric hindrance which could limit binding at the sensor interface. Though electrode surfaces are commonly depicted as planar surfaces, screen printed electrodes used are far from flat at the nanoscale. This irregular texture may prevent the analyte from binding to the receptor when is confined at the surface. The effect of steric hindrance has been previously identified as an issue in biosensor fabrication[23,30,44].

Whilst this study is far from field deployment, improvements such as the reduction of chip-to-chip variability in the electrodes and automated sensor construction techniques could create more reliable sensors and enable effective point-of use testing comparable to ELISA assays or similar in a more user-friendly format. Using the recognised system of 'technology readiness levels' [45], this work is currently at level 4-5, relatively nascent compared to the ELISA, a routine technique used in industry (level 9). This study has demonstrated for the fabrication of a sensitive and specific reagentless immunosensor using novel nanobody constructs. In addition to the advantages of using both unmodified and engineered nanobodies over polyclonal antibodies, this study presents insight relevant to the use of small binding proteins in electrochemical sensors, it is hoped that the lessons learnt in this study may inform the investigation of other NABP based sensors.

5 Acknowledgements

The author would like to thank the commercial support of Abcam Plc. for access to receptors. Thanks also go to BBSRC for project funding and C. Jackson & D. Langford for editorial assistance.

6 References

[1] E.C. Alocilja, S.M. Radke, Market analysis of biosensors for food safety, Biosens. Bioelectron. 18 (2003) 841–846. doi:10.1016/S0956-5663(03)00009-5.

[2] J.H.T. Luong, K.B. Male, J.D. Glennon, Biosensor technology: Technology push versus market pull, Biotechnol. Adv. 26 (2008) 492–500. doi:10.1016/j.biotechadv.2008.05.007.

[3] M.I. Prodromidis, Impedimetric immunosensors—A review, Electrochimica Acta. 55 (2010) 4227–4233. doi:10.1016/j.electacta.2009.01.081.

[4] P.B. Luppa, L.J. Sokoll, D.W. Chan, Immunosensors - principles and applications to clinical chemistry, Clin. Chim. Acta. 314 (2001) 1–26. doi:10.1016/s0009-8981(01)00629-5.
[5] X. Zeng, Z. Shen, R. Mernaugh, Recombinant antibodies and their use in biosensors, Anal. Bioanal. Chem. 402 (2012) 3027–3038. doi:10.1007/s00216-011-5569-z.
[6] L. Kummer, C.-W. Hsu, O. Dagliyan, C. MacNevin, M. Kaufholz, B. Zimmermann, et al., Knowledge-Based Design of a Biosensor to Quantify Localized ERK Activation in Living Cells, Chem. Biol. 20 (2013) 847–856. doi:10.1016/j.chembiol.2013.04.016.
[7] C. Tiede, A.A. Tang, S.E. Deacon, U. Mandal, J.E. Nettleship, R.L. Owen, et al., Adhiron: a stable and versatile peptide display scaffold for molecular recognition applications, Protein Eng Sel. 27 (2014) 145–55. doi:10.1093/protein/gzu007.
[8] C. Grönwall, S. Ståhl, Engineered affinity proteins—Generation and applications, J. Biotechnol. 140 (2009) 254–269. doi:10.1016/j.jbiotec.2009.01.014.
[9] F.F. Miranda, E. Brient-Litzler, N. Zidane, F. Pecorari, H. Bedouelle, Reagentless fluorescent biosensors from artificial families of antigen binding proteins, Biosens. Bioelectron. 26 (2011) 4184–4190. doi:10.1016/j.bios.2011.04.030.
[10] H. Li, J. Yan, W. Ou, H. Liu, S. Liu, Y. Wan, Construction of a biotinylated cameloid-like antibody for lable-free detection of apolipoprotein B-100, Biosens. Bioelectron. 64 (2015) 111–118. doi:10.1016/j.bios.2014.08.060.
[11] E. De Genst, D. Saerens, S. Muyldermans, K. Conrath, Antibody repertoire development in camelids, Dev. Comp. Immunol. 30 (2006) 187–198. doi:10.1016/j.dci.2005.06.010.
[12] L. Huang, S. Muyldermans, D. Saerens, Nanobodies® proficient tools in diagnostics, Expert Rev. Mol. Diagn. 10 (2010) 777–785. doi:10.1586/erm.10.62.
[13] C. Vincke, S. Muyldermans, Introduction to heavy chain antibodies and derived Nanobodies, Methods Mol Biol. 911 (2012) 15–26. doi:10.1007/978-1-61779-968-6_2.
[14] P. Schotte, P. Stanssens, C. Labeur, J.L. Jonniaux, M.J. Lauwereys, Method for the production of domain antibodies, (2012). https://www.google.com/patents/US20120157664.
[15] S. Muyldermans, T.N. Baral, V.C. Retamozzo, P. De Baetselier, E. De Genst, J. Kinne, et al., Camelid immunoglobulins and nanobody technology, Vet. Immunol. Immunopathol. 128 (2009) 178–183. doi:10.1016/j.vetimm.2008.10.299.
[16] A.Q. Abbady, A. Al-Mariri, M. Zarkawi, A. Al-Assad, S. Muyldermans, Evaluation of a nanobody phage display library constructed from a Brucella-immunised camel, Vet. Immunol. Immunopathol. 142 (2011) 49–56. doi:10.1016/j.vetimm.2011.04.004.
[17] M. Behdani, S. Zeinali, M. Karimipour, H. Khanahmad, S. Schoonooghe, A. Aslemarz, et al., Development of VEGFR2-specific Nanobody Pseudomonas exotoxin A conjugated to provide efficient inhibition of tumor cell growth, New Biotechnol. 30 (2013) 205–209. doi:10.1016/j.nbt.2012.09.002.
[18] G. Hassanzadeh-Ghassabeh, N. Devoogdt, P. De Pauw, C. Vincke, S. Muyldermans, Nanobodies and their potential applications, Nanomedicine Lond. 8 (2013) 1013–26. doi:10.2217/nnm.13.86.
[19] S. Oliveira, R. Heukers, J. Sornkom, R.J. Kok, P.M.P. van Bergen en Henegouwen, Targeting tumors with nanobodies for cancer imaging and therapy, J. Controlled Release. 172 (2013) 607–617. doi:10.1016/j.jconrel.2013.08.298.
[20] H.J.J.W. De, E. Dolk, M.J.S. Saunders, Anti-fc-receptor single domain antibodies (nanobodies-tm) and therapeutic use, (2009). https://www.google.com/patents/EP2102243A2?cl=en.
[21] T. De Meyer, S. Muyldermans, A. Depicker, Nanobody-based products as research and diagnostic tools, Trends Biotechnol. (n.d.). doi:10.1016/j.tibtech.2014.03.001.
[22] T. Fodey, P. Leonard, J. O'Mahony, R. O'Kennedy, M. Danaher, Developments in the production of biological and synthetic binders for immunoassay and sensor-based detection of small molecules, TrAC Trends Anal. Chem. 30 (2011) 254–269. doi:10.1016/j.trac.2010.10.011.
[23] B. Lu, M.R. Smyth, R. O'Kennedy, Oriented immobilization of antibodies and its applications in immunoassays and immunosensors, Analyst. 121 (1996) 29R–32R.

[24] J. Mitchell, Small Molecule Immunosensing Using Surface Plasmon Resonance, Sensors. 10 (2010) 7323–7346. doi:10.3390/s100807323.
[25] B. Piro, S. Reisberg, V. Noel, M.C. Pham, Investigations of the steric effect on electrochemical transduction in a quinone-based DNA sensor, Biosens. Bioelectron. 22 (2007) 3126–3131. doi:10.1016/j.bios.2007.02.007.
[26] D. Hanahan, STUDIES ON TRANSFORMATION OF ESCHERICHIA-COLI WITH PLASMIDS, J. Mol. Biol. 166 (1983) 557–580. doi:10.1016/s0022-2836(83)80284-8.
[27] T. Honda, Y. Akahori, Y. Kurosawa, Method of constructing camel antibody library, (2003). https://www.google.com/patents/WO2003025020A1?cl=en.
[28] M. Gerard, A. Chaubey, B.D. Malhotra, Application of conducting polymers to biosensors, Biosens. Bioelectron. 17 (2002) 345–359. doi:10.1016/s0956-5663(01)00312-8.
[29] A.V. Pournaras, T. Koraki, M.I. Prodromidis, Development of an impedimetric immunosensor based on electropolymerized polytyramine films for the direct detection of Salmonella typhimurium in pure cultures of type strains and inoculated real samples, Anal. Chim. Acta. 624 (2008) 301–307. doi:10.1016/j.aca.2008.06.043.
[30] M.M. Billah, C.S. Hodges, H.C.W. Hays, P.A. Millner, Directed immobilization of reduced antibody fragments onto a novel SAM on gold for myoglobin impedance immunosensing, Bioelectrochemistry. 80 (2010) 49–54. doi:10.1016/j.bioelechem.2010.08.005.
[31] G.T. Hermanson, Bioconjugate Techniques, Academic Press, 2008.
[32] A.J. Bard, L.R. Faulkner, Electrochemical Methods, John Wiley & Sons, 2001.
[33] B. Corry, J. Uilk, C. Crawley, Probing direct binding affinity in electrochemical antibody-based sensors, Anal. Chim. Acta. 496 (2003) 103–116. doi:10.1016/j.aca.2003.01.001.
[34] G. Farace, G. Lillie, T. Hianik, P. Payne, P. Vadgama, Reagentless biosensing using electrochemical impedance spectroscopy, Bioelectrochemistry. 55 (2002) 1–3. doi:10.1016/S1567-5394(01)00166-9.
[35] J.G. Guan, Y.Q. Miao, Q.J. Zhang, Impedimetric biosensors, J. Biosci. Bioeng. 97 (2004) 219–226. doi:10.1016/s1389-1723(04)70195-4.
[36] G. Lillie, P. Payne, P. Vadgama, Electrochemical impedance spectroscopy as a platform for reagentless bioaffinity sensing, Sens. Actuators B Chem. 78 (2001) 249–256. doi:10.1016/S0925-4005(01)00821-8.
[37] A. Ahmed, J.V. Rushworth, J.D. Wright, P.A. Millner, Novel Impedimetric Immunosensor for Detection of Pathogenic Bacteria Streptococcus pyogenes in Human Saliva, Anal. Chem. (2013). doi:10.1021/ac403253j.
[38] M. Trojanowicz, T. Krawczyński vel Krawczyk, Electrochemical biosensors based on enzymes immobilized in electropolymerized films, Microchim. Acta. 121 (1995) 167–181. doi:10.1007/bf01248249.
[39] R.L. Caygill, C.S. Hodges, J.L. Holmes, S.P.J. Higson, G.E. Blair, P.A. Millner, Novel impedimetric immunosensor for the detection and quantitation of Adenovirus using reduced antibody fragments immobilized onto a conducting copolymer surface, Biosens. Bioelectron. 32 (2012) 104–110. doi:10.1016/j.bios.2011.11.041.
[40] R.B. Queirós, N. de-los-Santos-Álvarez, J.P. Noronha, M.G.F. Sales, A label-free DNA aptamer-based impedance biosensor for the detection of E. coli outer membrane proteins, Sens. Actuators B Chem. 181 (2013) 766–772. doi:10.1016/j.snb.2013.01.062.
[41] F. Darain, S.-U. Park, Y.-B. Shim, Disposable amperometric immunosensor system for rabbit IgG using a conducting polymer modified screen-printed electrode, Biosens. Bioelectron. 18 (2003) 773–780. doi:10.1016/S0956-5663(03)00004-6.
[42] M. Díaz-González, D. Hernández-Santos, M.B. González-García, A. Costa-García, Development of an immunosensor for the determination of rabbit IgG using streptavidin modified screen-printed carbon electrodes, Talanta. 65 (2005) 565–573. doi:10.1016/j.talanta.2004.07.022.
[43] V.F. Lvovich, Impedance Spectroscopy, Wiley, 2012.

[44] H. Zheng, X. Du, Reduced steric hindrance and optimized spatial arrangement of carbohydrate ligands in imprinted monolayers for enhanced protein binding, Biochim. Biophys. Acta BBA - Biomembr. 1828 (2013) 792–800. doi:10.1016/j.bbamem.2012.11.006.
[45] EARTO, The TRL Scale as a Research & Innovation Policy Tool, EARTO Recommendations, (2014). http://www.earto.eu/fileadmin/content/03_Publications/The_TRL_Scale_as_a_R_I_Policy_Tool_-_EARTO_Recommendations_-_Final.pdf (accessed April 15, 2016).

Author Biographies

Jack Goode

Jack Goode is currently working on the development of biosensors for colorectal disease at Leeds teaching Hospitals. He received his BSc. in Nanotechnology from University of Leeds in 2010 and PhD in Bionanotechnology in 2015 which was sponsored by BBSRC and Abcam Plc. He has previous research experience in biomaterials engineering and has worked in the public engagement and dissemination of research.

Gary Dillon

Gary Dillon is head of R&D at Abcam Plc. He obtained his BSc. in Biochemistry at York in 2002, going on to study a Ph.D. in parasitology also at York. He then went onto postdoctoral work before moving to the Wellcome trust Sanger institute. He has been working with Abcam since 2010 on the development of novel immune-reagents and assay development.

Paul Millner

Paul Millner directs the Bionanotechnology group at the University of Leeds. The group's interests can be divided broadly into two main themes: biosensors and nanotechnology. He initially trained as a biochemist and obtained his Ph.D. in plant sciences from the University of Leeds. Paul is also Director of the School of Biomedical Sciences and delivers lectures on a range of topics.

Fig. 1

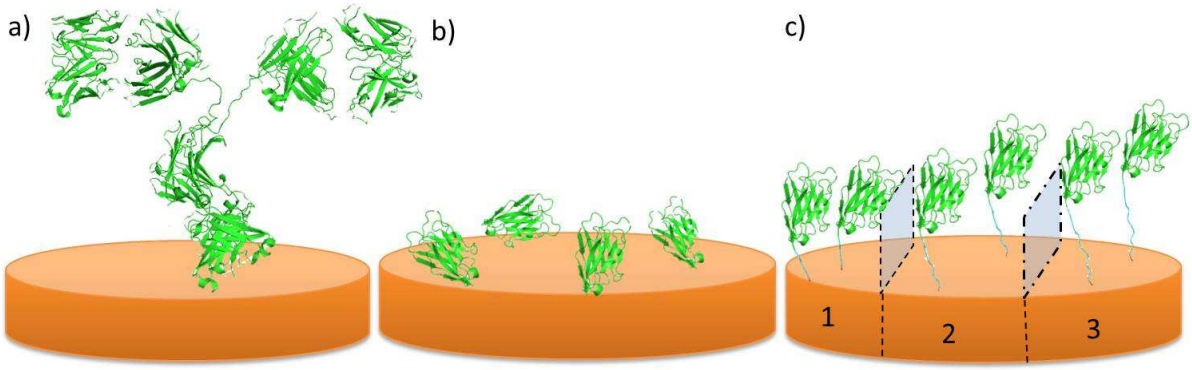

Figure 1: An Illustration of different bioreceptors used. Antibody based biosensors using full antibodies (a) and non-oriented (b) and oriented nanobody sensors with engineered peptide spacer (c) of 5, 10 and 15 amino acids, (1, 2 and 3 respectively). Figure is illustrative of the size difference between different receptors.

Fig. 2

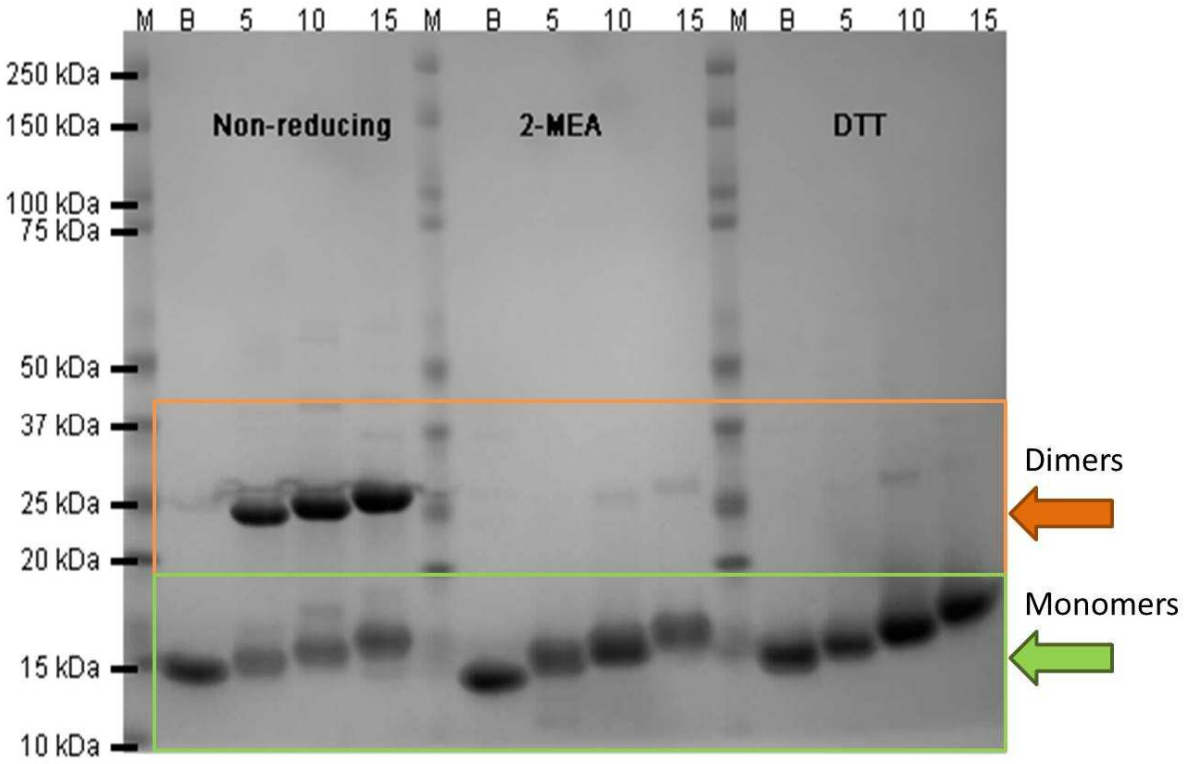

Figure 2: non reducing SDS-PAGE of nanobody dimers and monomers. Coomassie staining of a gel run using MES buffer. The gel shows the nanobody under non-reducing and fully reducing conditions (DTT). 2-MEA lanes shows successful reduction of dimers which were then running SDS-Page under non reducing conditions [M=marker, B= basic nanobody, with no cysteine modification, 5, 10 and 15 are nanobodies with respective peptide spacers]. Arrows indicate dimers and monomers respectively.

Fig. 3

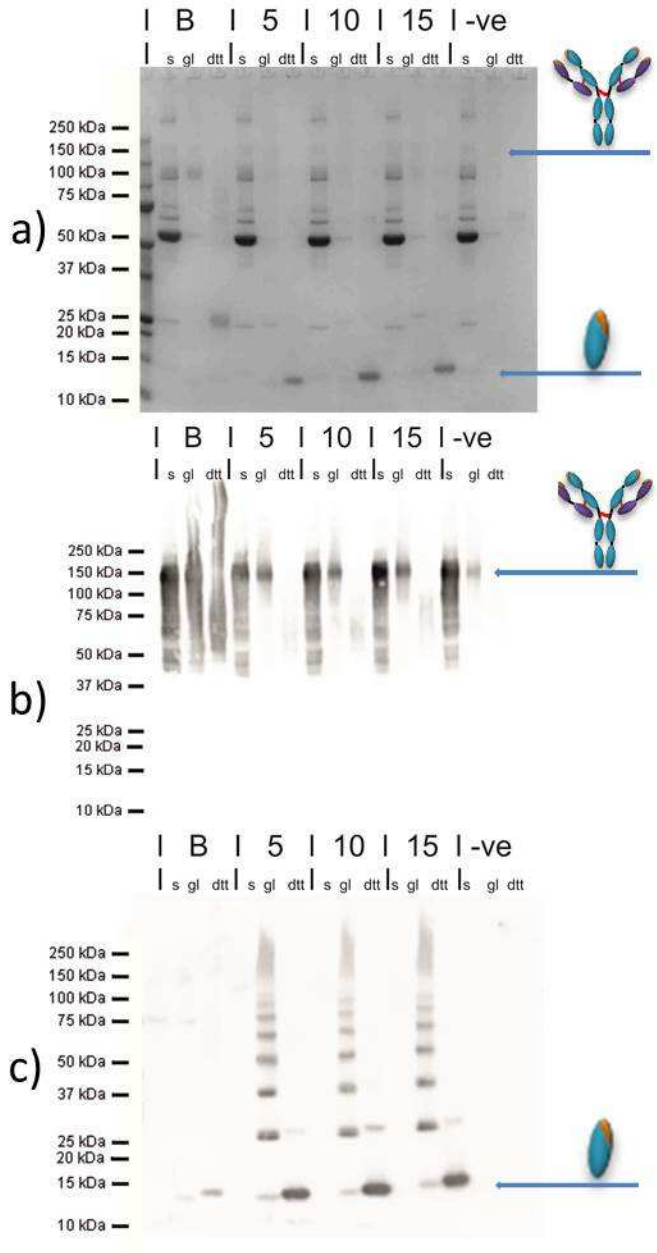

Figure 3: Coomassie stain (a) and immunoblot using anti rabbit IgG secondary (b) and anti his_6-tag secondary (c). Across all panels diluted sera (s) are compared with fractions yielded from IP elutions, both glycine (gl) and DTT (dtt) respectively. In each panel B, 5,10, 15 are the respective nanobody constructs with 5,10 and 15 amino acid spacer respectively alongside a non-specific control where Sulfolink®beads were blocked with buffer containing cysteine(-ve)

Fig. 4

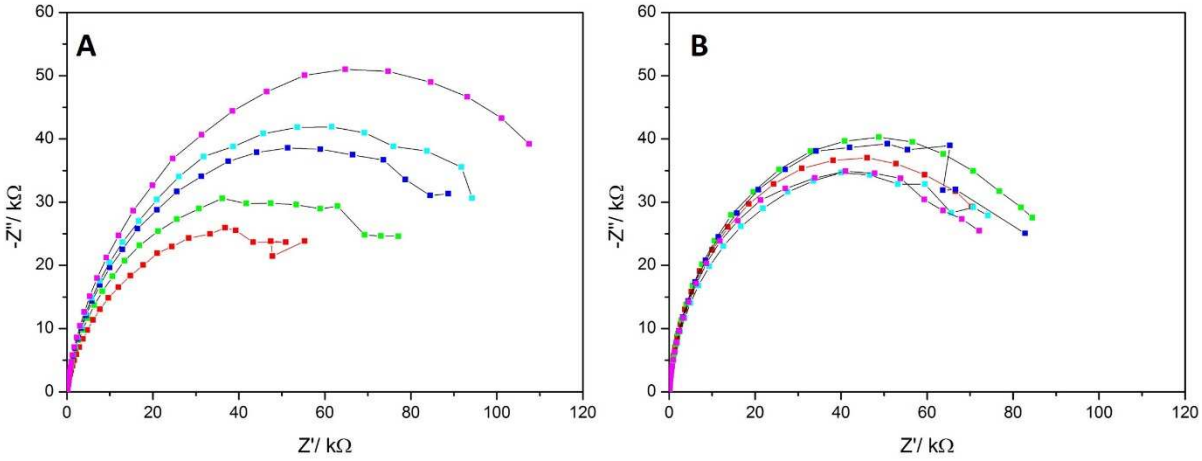

Figure 4: Plot of impedance Nyquist data for a nanobody biosensor to detect rabbit IgG analyte. a) with Rabbit IgG (+ve) b)With Sheep IgG(-ve) 0 nM —■—, 666 fM —●—, 6.66 pM —▲—666 pM —▼—, 666 nM —◆—. Illusrtrative data of one biosensor with nanobody bioreceptor with 5 amino acid spacer. Inset (B) shows the equivalent cell used to Simulate data and derive calibration values.

Fig. 5

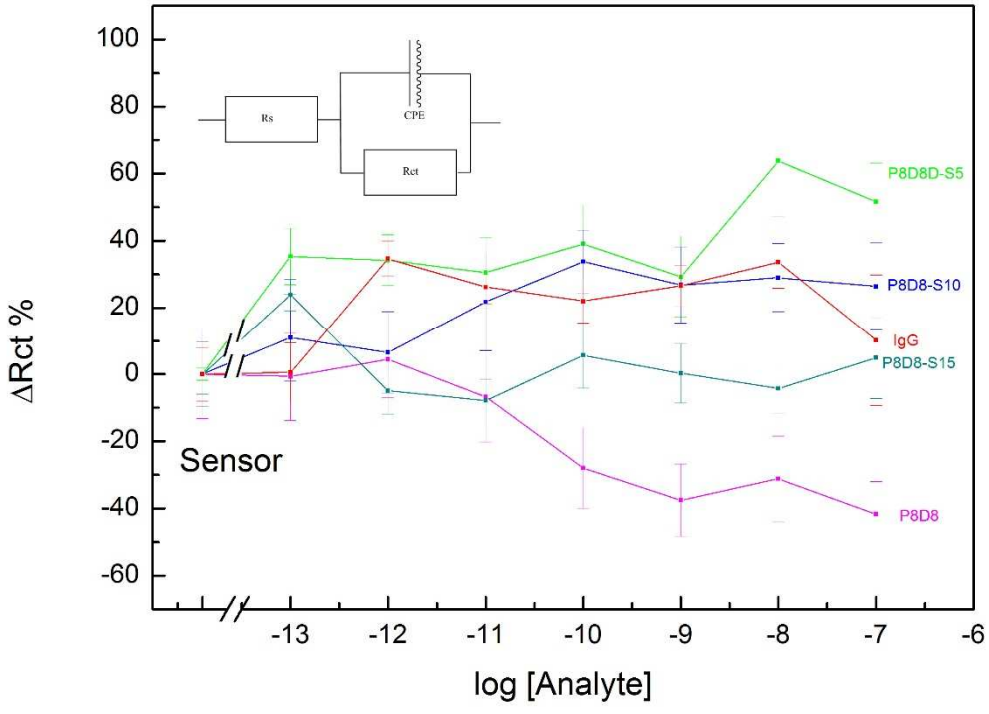

Figure 5: Comparison of analyte specific (total binding – non-specific binding) signal generated using different bioreceptor constructs (—■— P8D8; —■— P8D8-S5; —■— P8D8-S10; —■— P8D8-S15; —■— IgG.) (n=5±StdEr). Inset shows the equivalent cell used to simulate nyquist data and derive calibration values.

Fig. 6

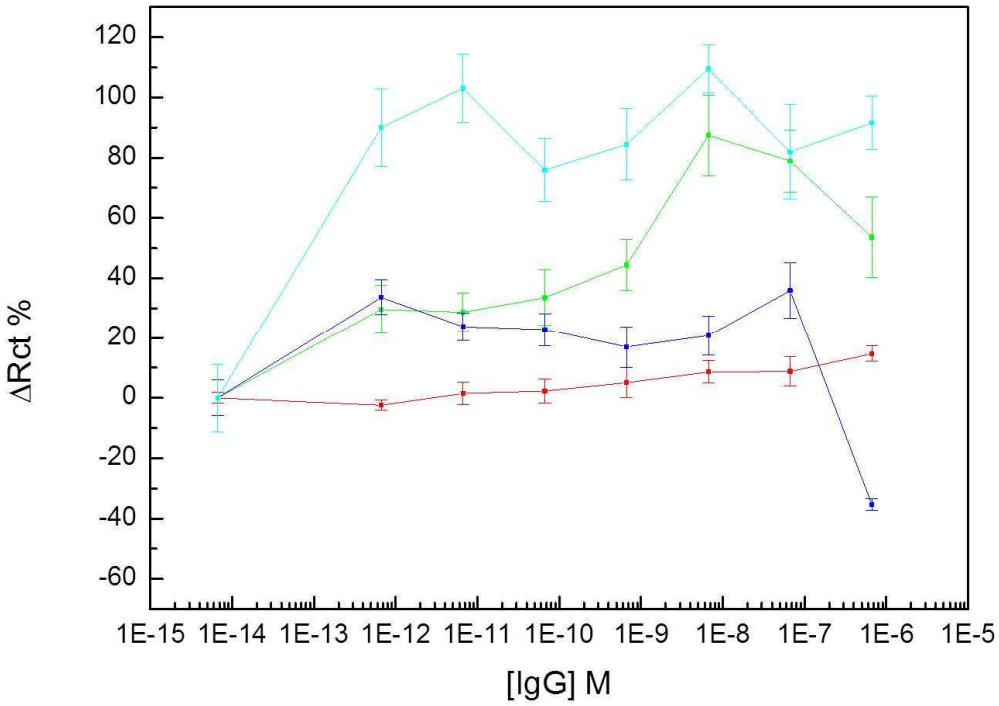

Figure 6: Performance of a biosensor for rabbit IgG constructed using five amino acid spacer (—■— rabbit IgG in 100% human sera; —■— rabbit IgG in PBS; —■— rabbit IgG in 10% human sera: PBS(v:v); —■— sheep IgG in PBS (-ve). (n=8±StdEr).